Title

Genomic analysis of distinct bleaching tolerances among cryptic coral species

Journal

Proceedings of the Royal Society B, 288(1960)

ISSN

0962-8452

Authors

Rose, Noah H
Bay, Rachael A
Morikawa, Megan K
et al.

Publication Date

2021-10-13

DOI

10.1098/rspb.2021.0678

Peer reviewed

PROCEEDINGS B

royalsocietypublishing.org/journal/rspb

Research

Cite this article: Rose NH, Bay RA, Morikawa MK, Thomas L, Sheets EA, Palumbi SR. 2021 Genomic analysis of distinct bleaching tolerances among cryptic coral species. *Proc. R. Soc. B* **288**: 20210678. https://doi.org/10.1098/rspb.2021.0678

Received: 19 March 2021
Accepted: 17 September 2021

Subject Category:
Evolution

Subject Areas:
evolution, genomics, ecology

Keywords:
coral bleaching, ecological genomics, cryptic species

Author for correspondence:
Noah H. Rose
e-mail: noahhrose@gmail.com

Electronic supplementary material is available online at https://doi.org/10.6084/m9.figshare.c.5647045.

THE ROYAL SOCIETY PUBLISHING

Genomic analysis of distinct bleaching tolerances among cryptic coral species

Noah H. Rose[1,5], Rachael A. Bay[2,5], Megan K. Morikawa[5], Luke Thomas[3,4,5], Elizabeth A. Sheets[5] and Stephen R. Palumbi[5]

[1]Department of Ecology and Evolutionary Biology, Princeton University, Princeton, NJ, USA
[2]Department of Evolution and Ecology, University of California, Davis, CA, USA
[3]The UWA Oceans Institute, The University of Western Australia, Perth, Western Australia, Australia
[4]Australian Institute of Marine Science, Perth, Western Australia, Australia
[5]Hopkins Marine Station, Stanford University, Pacific Grove, CA, USA

RAB, 0000-0002-9516-5881

Reef-building coral species are experiencing an unprecedented decline owing to increasing frequency and intensity of marine heatwaves and associated bleaching-induced mortality. Closely related species from the *Acropora hyacinthus* species complex differ in heat tolerance and in their association with heat-tolerant symbionts. We used low-coverage full genome sequencing of 114 colonies monitored across the 2015 bleaching event in American Samoa to determine the genetic differences among four cryptic species (termed HA, HC, HD and HE) that have diverged in these species traits. Cryptic species differed strongly at thousands of single nucleotide polymorphisms across the genome which are enriched for amino acid changes in the bleaching-resistant species HE. In addition, HE also showed two particularly divergent regions with strong signals of differentiation. One approximately 220 kb locus, HES1, contained the majority of fixed differences in HE. A second locus, HES2, was fixed in HE but polymorphic in the other cryptic species. Surprisingly, non-HE individuals with HE-like haplotypes at HES2 were more likely to bleach. At both loci, HE showed particular sequence similarity to a congener, *Acropora millepora*. Overall, resilience to bleaching during the third global bleaching event was strongly structured by host cryptic species, buoyed by differences in symbiont associations between these species.

1. Introduction

Reef-building corals live across strong environmental gradients and comprise many species with different levels of local adaptation (e.g. [1]). This is especially true for corals experiencing high water temperatures, which cause stress-induced breakdown of the ecologically vital symbiosis between the coral host and the dinoflagellate symbionts of the family *Symbiodinaceae* that provide most of the fixed carbon used by many coral species; this process is known as coral bleaching [2,3]. Heat-resistant individuals within species have been reported across latitudinal gradients [4,5] or across fine-scale mosaics of reef temperatures [1]. The genetics of these differences appear to involve many loci but the role and size of these effects are unknown [4,6].

If ecological trait differences are related to genetic variation at a small number of loci, then these traits can respond very quickly to strong selection imposed by environmental change, either by changes in the frequency of standing variation at major effect loci, or by introgression of these loci from other lineages—the latter process may play a particularly important role in species complexes spread across variable environments [7–11]. For example, the introgression of an aryl hydrocarbon receptor deletion from Atlantic to Gulf killifish enabled rapid adaptation to increased water pollution caused by humans [7]. Some loci of large effect may be constructed from many closely linked genes that respond as a single selective unit, sometimes referred to as 'supergenes'

[12–15]. For example, a supergene locus is associated with differences in wing patterning in *Heliconius* butterflies [16], and recent analyses suggest that introgression or differential assortment of ancestral variation in supergenes may have driven the rapid evolution of mimicry in different species [9,16,17]. Similarly, large regions of several chromosomes of the Atlantic cod show strong divergence and low recombination—these chromosomal regions are associated with strong fitness differences at different water temperatures [18]. However, a recent study found that bleaching resistance in the coral *Acropora millepora* has a polygenic basis, suggesting that large-effect loci may not enable a simple and rapid evolutionary response of corals in particular to climate change [19]. Overall, we still know very little about the genomic distribution, abundance and effect sizes of adaptive variants in natural populations, especially those with large ranges across environmental mosaics [20].

In recent years, coral bleaching has dramatically increased in incidence owing to the combined effects of cyclical climate variation and increasing ocean temperatures driven by greenhouse gas emissions [3,21]. The first described global coral bleaching event occurred during the 1998 El Niño; a second global bleaching event occurred in 2010. During the 2015–2016 El Niño, coral reefs around the world experienced high levels of bleaching associated with exceptionally high sea surface temperatures. This was the third major global bleaching event observed in recorded history [22].

During the 2015 bleaching event, we observed extensive coral bleaching in the backreef lagoon of Ofu, American Samoa. Tabletop corals of the *Acropora hyacinthus* species complex showed highly variable bleaching responses. This coral is closely related to its congener *A. millepora*, which has a high-quality sequenced genome [19]. Acroporid corals underwent a major adaptive radiation 2–3 Ma and are notable for their propensity to hybridize and their reticulate phylogenetic structure. Previous work has shown that four different cryptic species of *A. hyacinthus* are present on Samoan reefs (termed species HA, HC, HD and HE) [23,24]. These different species show important differences in ecology and stress tolerance. Species HE is broadly distributed across the Ofu backreef, and is abundant even in a thermally stressful lagoon pool, known as the highly variable pool, that experiences temperatures as high as 35°C [1]. Species HA, HC and HD are largely confined to a lagoon pool that experiences more consistent temperatures (moderately variable pool) [23,24]. Corals on the Ofu backreef host two different symbiont types, of the genera *Cladocopium* and *Durusdinium*; *Durusdinium* symbionts have been associated with more stressful environments and greater bleaching resistance [25,26]. We previously found evidence that among colonies of species HE and HC coexisting in the moderately variable pool, HE was more likely to host the stress-tolerant *Durusdinium* symbionts [24]. We used RNA sequencing to also show that a large number of genome-wide protein-coding differences are under selection between species HC and HE, despite very weak genetic differentiation across most of the transcriptome [24]. Associated with these differences in microhabitat distribution, host genetics and symbiont association, species HE shows increased tolerance to experimental heat stress and bleached less during the 2015 bleaching event than species HC [24]. Other cryptic coral species complexes have also been observed to harbour variation in environmental tolerance [27,28]; a deeper understanding of the genomic factors underlying cryptic species differences will play a key role in predicting the responses of coral reefs to rapid climate change.

Here, we expand the number of colonies assayed for each species and confirm that species HA, HC and HD all showed greater bleaching responses to the 2015 bleaching event; these effects were strongly associated with a lower propensity of these species to host *Durusdinium* symbionts. We use low-coverage genome-wide sequencing of 114 *A. hyacinthus* colonies to identify genomic regions showing strong divergence in the thermally resilient HE lineage and identify signatures of polygenic directional selection in the HE lineage. One locus is responsible for the vast majority (88%) of fixed differences between HE and the other cryptic species. We find that genetic structure at this locus and another strongly diverged but unfixed locus, along with symbiont associations, provide potentially useful genomic predictors of differences in bleaching outcomes.

2. Results

We used low-coverage (2×) whole-genome sequencing to assay genomic variation and symbiont associations across 50 bleached and 64 non-bleached coral colonies surveyed in the Ofu backreef in American Samoa (electronic supplementary material, figure S1). We mapped (quality score greater than 20) 741 076 617 paired-end 125 base-pair *A. hyacinthus* reads (approx. 100 gigabases) to the recently finished chromosome-scale *A. millepora* genome [19] and found 6 721 576 sites where the *A. hyacinthus* consensus differed from *the A. millepora* reference (1.4% divergence)—2 280 184 of these sites were fixed across *A. hyacinthus*, while the remaining 4 441 392 were polymorphic with a major allele (in a balanced panel containing 10 individuals of each cryptic species) that differed from the *A. millepora* reference. Incorporating these bases into a new reference, we were able to increase the number of reads with high-quality mapping (quality score greater than 20) to 763 684 010 (a 1% increase). Comparing *A. hyacinthus* reads to one another at sites with 1–4 × mean coverage across samples, we found 16 210 139 single nucleotide polymorphisms (SNPs) with minor allele frequency (MAF) greater than 5% among our 114 samples; SNP MAFs were inferred by maximum likelihood (see Methods).

(a) Cryptic species identity, symbiont associations and bleaching

We found that all of the sampled colonies of *A. hyacinthus* could be assigned to one of four cryptic species (13 HA, 23 HC, 26 HD and 52 HE individuals, respectively): we did not see evidence of hybrid ancestry for any individuals (figure 1*a*). Principal component analysis (PCA) of genome-wide SNPs confirmed that colonies formed four tight clusters with no colonies falling in intermediate positions (figure 1*b*). Among the 23 colonies that had previously been assigned to cryptic species using Sanger sequencing-based multilocus genotyping [23], the new genome-wide assignments agreed with the previous assignments in all but one case, an individual that was previously assigned to species HA but was assigned to species HC in the present analysis (electronic supplementary material, table S1).

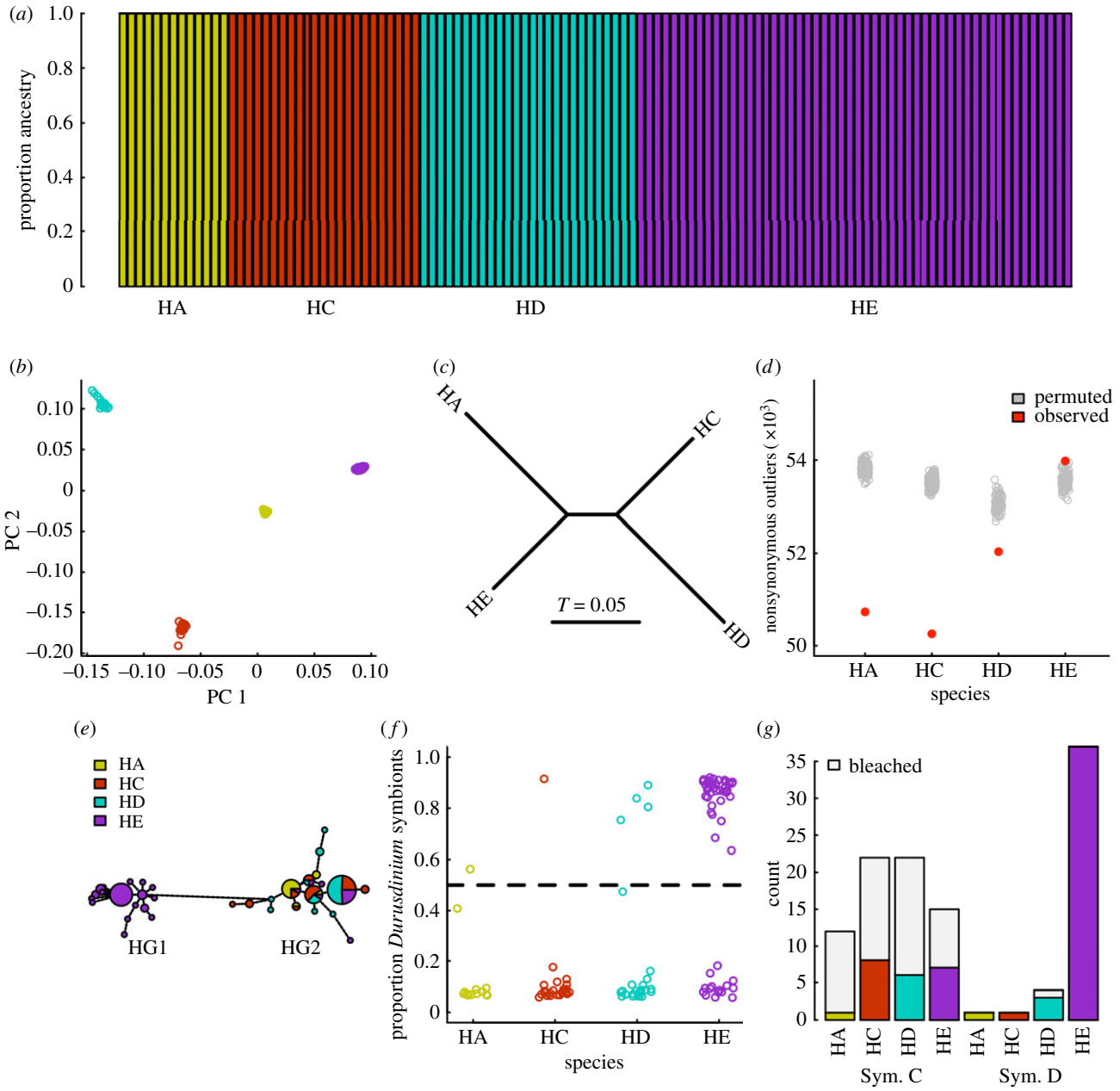

Figure 1. (*a*) Barplot of the proportion of *NGSadmix*-derived cryptic species ancestry for each of 114 colonies of *Acropora hyacinthus*. (*b*) PCA of the 114 colonies shows that the colonies form four distinct clusters, with no intermediate samples. Colours correspond to (*a*). (*c*) Neighbour-joining tree of cryptic species, where $T = -\log(1\text{-}F_{ST})$. (*d*) Observed versus permuted number of missense SNPs in the top 10% of species-specific allele frequency shifts. HA, HC and HD show evidence of constraint, while HE shows evidence of genome-wide selection for protein-coding change. (*e*) Mitochondrial haplotype network of all 114 samples. Haplogroup 1 (HG1) contains only species HE, but haplogroup 2 (HG2) contains members of all four species. (*f*) Symbiont associations (proportion *Durusdinium*, where 0 represents only *Cladocopium* symbionts) for all colonies, broken up by cryptic species. (*g*) Bleaching outcomes for all combinations of cryptic species and majority symbiont type. Bleached individuals (greater than 10% colony bleached) are represented by grey bars whereas coloured bars represent tolerant individuals for each species. (Online version in colour.)

We found that the four cryptic species were weakly diverged across much of the genome and showed reticulate phylogenetic structure: mean pairwise F_{ST} between species was 0.15. Although species HA and HE were grouped separately from species HC and HD in a neighbour-joining tree based on genome-wide F_{ST} (figure 1*c*), neighbour-joining trees from individual 10 kb windows across the genome showed all three possible tree topologies were commonly found (electronic supplementary material, figure S1).

In order to test for genome-wide signatures of protein-coding evolution, we annotated predicted synonymous and nonsynonymous-coding sequence variants (electronic supplementary material, table S2). We sought to use a modified version of the McDonald-Krietman test [29], which tests for differences in the proportion of nonsynonymous variants among fixed and polymorphic variants; however, because there were very few fixed differences between species we instead used a permutation test to shuffle synonymous and nonsynonymous annotations and test whether our true set of nonsynonymous variants were more or less likely than frequency-matched permuted sets to show lineage-specific shifts in allele frequencies (see Methods). We found that for cryptic species HA, HC and HD, nonsynonymous variants were much less likely to be in the top 10% of genome-wide population branch statistics (PBS) than in our permutations ($p < 0.01$) consistent with a widespread selective constraint

on protein sequences in these species (figure 1*d*; electronic supplementary material, figure S2). However, for cryptic species, HE we saw the opposite pattern: there were about 500 more nonsynonymous outliers than we expected from our permutation analysis ($p < 0.01$), consistent with pervasive selection for protein-coding change across many genes in this lineage. However, other processes besides selection on adaptive variants could also explain these results; for example, if HE has experienced periods of low effective population size, selection against mildly deleterious nonsynonymous variants could be relaxed in this lineage [30]. We saw a similar pattern using a 5% cutoff. However, using a 1% cutoff the pattern differed somewhat: HA and HC still showed signatures of constraint, but for HD, there were now about 100 more outlier nonsynonymous variants than expected under neutrality. For HE, nonsynonymous variants were neither more or less likely than synonymous variants to be 1% outliers (electronic supplementary material, figure S2). Overall, these results suggest that protein sequences across the genome are under typical selective constraint in HA and HC. HD and HE both show signs of genome-wide selection for protein-coding change (or relaxed selection against this change), though in HE this signal involves a larger number of SNPs. These patterns are subtle but indicate that small differences in allele frequencies across the genome may play a role in generating functional differences between cryptic species.

Mitochondrial genomes also showed strong structure between HE and other cryptic species; one haplotype cluster (HG1, figure 1*e*) only contained individuals of cryptic species HE, while the other cluster (HG2, figure 1*e*) contained individuals of all four cryptic species. Mitochondrial haplotypes didn't differ according to pool (highly variable pool: three HG1, eight HG2; moderately variable pool nine HG1, 32 HG2). Mitochondrial incongruence with nuclear data has previously been observed in Acroporid corals and probably reflects the complex history of speciation in this genus [11,31].

Cryptic species differed strongly in their propensity to host thermally tolerant genus *Durusdinium* symbionts (figure 1*f*). In the cooler, moderately variable pool, the majority of HE corals (27 out of 41) contained greater than 50% genus *Durusdinium* symbionts, as measured by sequence depth, while only a minority of colonies of the other cryptic species hosted greater than 50% *Durusdinium* (HA: 1 out of 13, HC: 0 out of 22, HD: 2 out of 23). *Durusdinium* was more dominant in among HE colonies in the warmer, highly variable pool where 10 out of 11 colonies hosted mostly *Durusdinium.* Few colonies of the other species survive long in the highly variable pool, probably because of the higher maximum temperatures there [32], but these tended to have *Durusdinium* as well (two of three HD colonies and the single HC colony (see also [24,25,33]).

In parallel, cryptic species HE bleached much less than HA, HC or HD. Some of this effect was associated with the greater propensity of HE to host *Durusdinium* (figure 1*g*); for example, in the highly variable pool, the single colony of HE that bleached hosted *Cladocopium* symbionts instead of *Durusdinium.* Likewise, none of the HE in the moderately variable pool with *Durusdinium* bleached (0 out of 27), but 7 out of 14 of the HE colones with *Cladocopium* did (electronic supplementary material, table S1). Nevertheless, colonies of HA, HC and HD with *Cladocopium* bleached more than HE with *Cladocopium* (HA: 11 out of 12, HC: 14 out of 22, HD: 15 out of 21, likelihood ratio test $p = 0.035$).

In summary, species HE shows signs of selection on divergent SNPs at hundreds of loci, in contrast with the other cryptic species, is much more likely to host heat-tolerant *Durusdinium* symbionts, and even when hosting *Calodocopium* symbionts is less likely to bleach.

(b) Genomic distribution of cryptic species differences

We next tested for the presence of regions of genomic differentiation between cryptic species that could be related to the observed differences in symbiont associations and bleaching outcomes. We calculated F_{ST} between each species pair in 10 kb windows and calculated mean PBS for each species in each window (see Methods and the electronic supplementary material, figure S2). We then calculated mean branch lengths across 100 kb windows with a step size of 10 kb across the genome. This approach allowed us to identify extended regions of differentiation between cryptic species while maintaining short-range patterns of linkage disequilibrium in our permutations. We identified several regions of differentiation with higher than expected levels of divergence (permutation false discovery rate (FDR) less than 0.05; electronic supplementary material, figure S3) within each species. In the following, we focused on the two peaks that differentiated species HE, because this species was most resistant to bleaching (figure 2*a*).

Despite low differentiation between cryptic species across most of the genome (mean pairwise $F_{ST} = 0.15$, see above), one locus on chromosome 7 from 20.35 to 20.57 Mb (HES1) in particular showed strong differentiation between HE and the other cryptic species; 1309 of 1483 SNPs (88%) putatively fixed or near-fixed (F_{ST} greater than 0.99) between HE and the three other cryptic species were found within this locus. One other locus on the unplaced scaffold Sc0000015 from 2.38 to 2.58 Mb also showed strong differentiation between HE and the other three cryptic species (HES2, figure 2*a*), but did not contain any fixed or near-fixed SNPs.

Because these regions of differentiation were detected on the basis of differences in F_{ST} between species, they reflect differences in the proportion of genetic diversity explained by species identity and not absolute differentiation. Accordingly, these signals could be driven by either increases in absolute differentiation (π_b) associated with reduced gene flow between species at these loci, or by decreases in nucleotide diversity (π_w) associated with selective sweeps or background selection in regions with low recombination rates. We plotted π_w in 100 kb sliding windows with a 10 kb step to assess the contribution of decreased diversity to the observed signal (electronic supplementary material, figure S7) [8]. We found that HES1 showed π_w at levels similar to the genome-wide average in species HE. These results imply selection against gene flow between species at this locus.

However, the other outlier region, HES2, showed a strong reduction in π_w in HE (electronic supplementary material, figure S7). These observations suggest that HES2 may have experienced lineage-specific, hard selective sweeps or background selection combined with low recombination rates, but may not have experienced strong selection against gene flow [34]. Tajima's D and Fay and Wu's H statistics further supported these interpretations—negative values of both of these statistics (corresponding to an excess of rare variation and an excess of high-frequency derived variants,

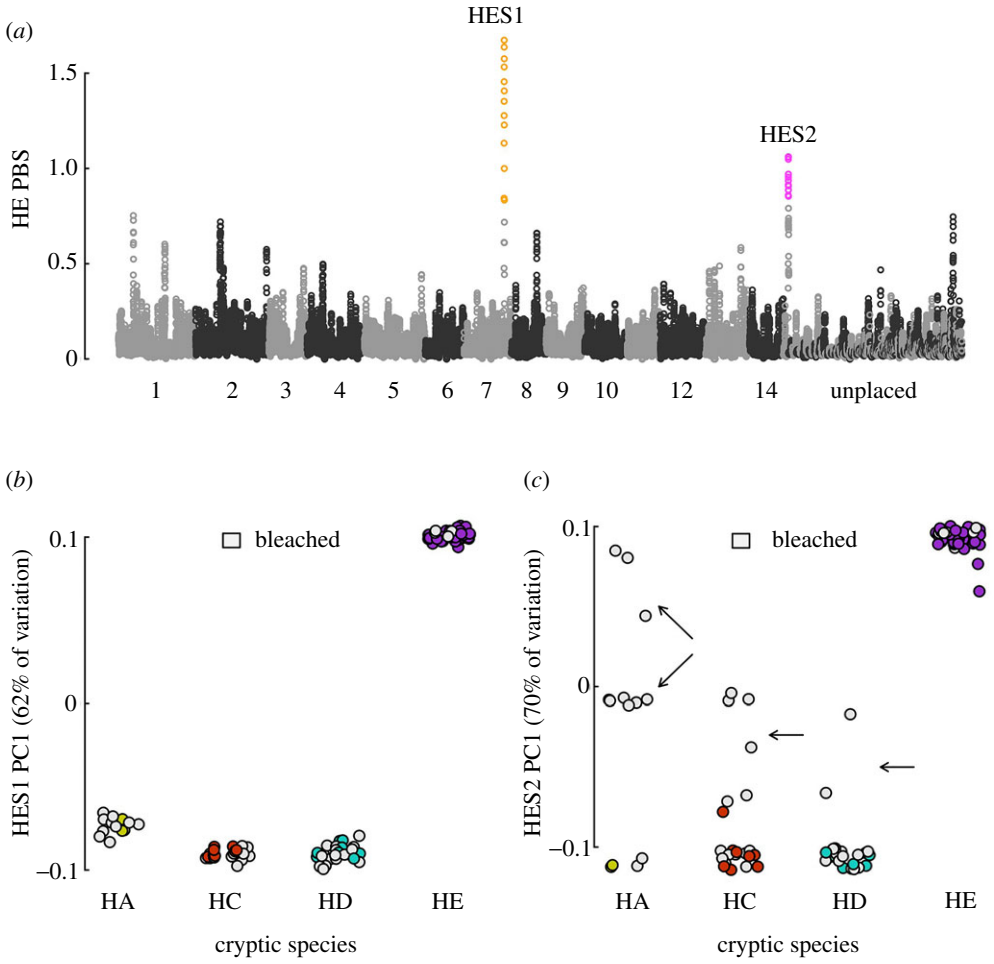

Figure 2. (*a*) The PBS (see Methods) in 100 kb windows with 10 kb step across the genome. Windows with FDR less than 0.05 are coloured by scaffold, and windows with FDR greater than 0.05 are coloured grey. Two loci (HES1 and HES2) show particularly strong differentiation. (*b*,*c*) Sample loadings onto the first principal component (PC1) computed across each locus, broken up by cryptic species. Bleached samples are shown in light grey. Arrows indicate non-HE corals with HE-like genotypes at HES2, all of which bleached. (Online version in colour.)

respectively) in both outlier regions in species HE are consistent with recent selective sweeps in HE in these regions (electronic supplementary material, figure S4 [35,36]).

(c) Analysis of divergent loci

We sought to further dissect the loci that showed the strongest differentiation between HE and the other cryptic species. HES1 contained two particularly strong peaks of differentiation between HE and the other cryptic species, one at 20.45 Mb and one at 20.51 Mb (electronic supplementary material, figure S8a). This locus contained 16 genes within its immediate vicinity, but most (9 out of 16) did not belong to known orthology groups. The annotated genes included a putative orthologue of solute carrier family 11 (SLC11A2), an RNA-binding motif protein (RBM48), DPY19L1, a proteasomal subunit (PSDM11), an E3 ubiquitin ligase (BRCA1), a MAP kinase (ZAK) and a NACHT and WD repeat domain-containing protein (NWD1). PSDM11, in particular, was located close to the highest peak of differentiation, although two uncharacterized proteins were also near this peak (electronic supplementary material, figure S8a). A *blastp* search suggested that one of these uncharacterized proteins (gene 12 598) may be a previously unannotated cytochrome oxidase 7A-like protein (best-annotated match, *Struthio camelus australis*, *E*-value = 0.14). HES1 contained 416 nonsynonymous SNPs, 120 of which were in the top 5% of genome-wide SNP branch lengths. Nonsynonymous SNPs were no more likely than synonymous SNPs to be in the top 5% of genome-wide branch lengths within HES1 (Fisher's exact test odds ratio = 1.1, p=0.52), but the high number of nonsynonymous SNPs suggests that this region of the genome harbours important functional diversity. We identified 49 nonsynonymous SNPs that were fixed or near-fixed between HE and the other cryptic species (F_{ST} greater than 0.99 between HE and all other species). Remarkably, 31 of these fixed nonsynonymous differences were concentrated in a single gene, the uncharacterized gene 12 599 (electronic supplementary material, figure S8a). An additional nine putatively fixed nonsynonymous differences were in the nearby uncharacterized gene 12 602. Both of these genes were located in HES1.

Given the strong divergence in protein sequences in genes 12 599 and 12 602, we sought to clarify the evolution of protein sequences in the *A. hyacinthus* complex relative to *A. millepora*. We were surprised to find that both predicted HE proteins were very similar to the *A. millepora* sequences, and that both species were strongly divergent from HA, HC and HD at these two loci (figure 3*a–d*). This pattern is very different from what is seen across the rest of the genome, where all *A. hyacinthus* cryptic species form an approximate polytomy and *A. millepora* is similarly divergent from all four (figure 3*e*,*f*). Given the large number of substitutions relative to *A. millepora*

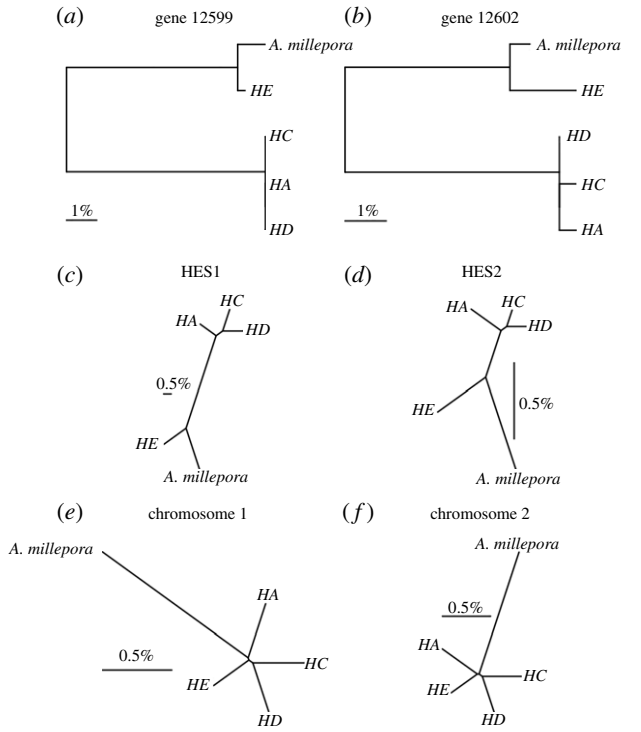

Figure 3. (*a*,*b*) Genes 12 599 and 12 602 show divergent protein sequences in HE; these sequences are more like *A. millepora* than HA, HC or HD. (*c*,*d*) In a neighbour-joining tree from nucleotide divergence, HE has a millepora-like sequence across HES1, and to a lesser extent across HES2. (*e*,*f*) The patterns seen across HES1 and HES2 are not typical of the rest of the genome, for example, across chromosomes 1 and 2.

and HE, it is possible that gene 12 599 has been pseudogenized in HA, HC and HD; otherwise its function may have been substantially altered. In a previous study, gene 12 599 was expressed at very low levels in both species HC and HE, with zero or one reads mapping in any given library [24]; this observation doesn't provide strong evidence for or against pseudogenization.

HES2 contained 15 genes in its immediate vicinity, five of which were annotated (electronic supplementary material, figure S8b). These included two ribosomal proteins (RPL3 and MRPS24), an NADH-ubiquinone oxidoreductase subunit 10 (NDUFA10), a protein containing a MULE transposase-like domain (MULE) and a putative TATA element modulatory factor (TMF1). HE sequences for HES2 were about as divergent from HA, HC and HD as they were from *A. millepora* (figure 3*d*).

(d) Genotypes and bleaching phenotypes

We next tested whether these loci, which were identified by their divergence between species, could help explain differences in bleaching outcomes within species. We used PCA to summarize and visualize genetic variation at each locus. As expected, because it is nearly fixed in HE, the first principal component (PC) of HES1 clearly separated HE from the three other species, which all clustered together (figure 2*b*). HES2 also separated HE from the other three species, but there were varied levels of differentiation from HE (figure 2*c*). In particular, some HA colonies clustered with species HE on PC axis 1, and other HA colonies were precisely intermediate. By contrast, HC and HD showed more continuous variation.

Because some of the coral colonies from a previous gene expression study were represented in the present study [24], we were able to compare individual expression levels from corals growing in a common environment (the moderately variable pool) with genetic variation across HES1 and HES2 (PC1 across each locus). Four genes in or near HES1 were differentially expressed between HC and HE in the previous study, but we could not assess within-species variation at this locus because of its lack of genomic variability within species (figure 2*b*). This same previous study had found that HC and HE have different levels of TMF1 expression—here we found that genetic variation across HES2 was correlated with TMF1 expression ($r = 0.84$). This pattern was seen between species, but also within: HC individuals with intermediate HE-like genotypes had intermediate expression (electronic supplementary material, figure S5). Because we have relatively few samples represented, it is difficult to remove potential trans-regulatory differences between the species (after correcting for species, the HES2 effect is not significant, ANOVA $p = 0.27$). However, these results suggest that future gene expression analyses including more coral colonies could provide clearer insights into the effects of this locus.

Unexpectedly, nearly all of the non-HE colonies with HE-like loadings on PC1 for HES2 bleached (17 out of 18; figure 2*c*) while bleaching of HE colonies with similar loadings was rare (8 out of 52). The SNPs that drove this signal were distributed across the locus, making it difficult to determine if these effects were associated with a particular gene (electronic supplementary material, figure S5A). However, this observation is confounded with the higher prevalence of *Durusdinium* symbionts among HE colonies. After correcting for cryptic species, symbiont differences and pool of origin, we found that HES2 genotype explained a significant additional amount of variation in bleaching (likelihood ratio test $p = 0.0006$). Although this analysis cannot definitively associate these loci with bleaching resilience, their strong differentiation between species in combination with their predictive power in this dataset and the weak structure observed across the rest of the genome suggests that they may play an important role in structuring variation within this species complex. Oddly, the association between HES2 and bleaching within species is the opposite of what would be expected from its distribution among cryptic species. Genotypes that were more similar to HE (the least bleaching-susceptible species) were associated with more bleaching in HA and HC (figure 2*c*).

(e) Genomic basis of symbiont associations

Because cryptic species differed strongly in symbiont associations, but symbiont associations were also variable within species HE, we tested whether any genomic loci were associated with differences in symbiont associations (electronic supplementary material, figure S6A). We did not detect substantial genetic differentiation between HE individuals that hosted different genera of symbionts, except in one small unplaced scaffold (xfSc0000366). However, this scaffold had high coverage in *Cladocopium*-dominated colonies and minimal coverage in *Durusdinium*-dominated colonies (electronic supplementary material, figure S6B). It is possible that genetic variation at this locus could enhance the acquisition or maintenance of *Durusdinium*. However, a likely alternative explanation is that this association represents an assembly or alignment artefact, and that xfSc0000366 is a *Cladocopium* locus.

3. Discussion

(a) Architecture of cryptic species differences in *Acropora hyacinthus*

We used whole-genome low-coverage population resequencing to show genome-wide patterns of differentiation across thousands of SNPs scattered throughout the genomes of cryptic species of coral that differ strongly in their response to high temperatures and natural bleaching events. In particular, the bleaching-resistant species HE shows a strong signal of amino acid change among divergent SNPs (figure 1*d*), as well as fixation or near fixation of hundreds of SNPs at two particularly divergent loci (figure 2*a*). A previous study found similar coding gene signals between HC and HE [24], but could not determine whether higher levels of amino acid evolution was driven by allele frequency changes in HC, HE or both. The present analysis using phylogenetic patterns of two additional species shows that this signal was driven by a pervasive protein-coding change in species HE and also shows a similar signal at other loci in species HD.

Cryptic species assignment revealed that we sampled uneven numbers of each species in this study (13 HA, 23 HC, 26 HD and 52 HE individuals), probably because it was carried out in a stressful backreef environment that may favour species HE. Further genomic studies in other habitats, including across forereefs, could increase our understanding of the distributions of and diversity within the different cryptic species.

(b) Evolution of highly divergent loci

One locus (HES1) showed particularly strong differentiation, including most of the fixed differences we observed across the entire genome between HE and the other species, suggesting that gene flow between *A. hyacinthus* species is limited and selection is strong at this locus [14,34]. The strongest signal of differentiation in HES1 occurred in several unannotated proteins and a region near a 26S proteasome non-ATPase regulatory subunit 11 (PSMD11). The 26S proteasome regulates the digestion of misfolded or damaged proteins after cellular stress, apoptosis and DNA damage repair. Transcription in many subunits of this complex is highly sensitive to temperature and increases about twofold 3 h after heat stress in HE [37]. A previous study found that *A. millepora* chromosomes 5 and 10 responded to selection for larval thermal tolerance; HES1 was found on chromosome 7, and so probably does not represent either of the loci identified in that study [4].

Immediately downstream of HES2 (and in a high-PBS window) was a putative TMF, thought in model systems to be involved in Golgi structure and tethering of vesicles and in regulation of a number of nuclear transcription factors [38,39]. It is highly upregulated 5 h after heat stress [40] and shows up to threefold higher expression in species HE than in HC [24]. We found that HES2 genotype was correlated with TMF expression, and that HC corals with intermediate HE-like genotypes had intermediate expression (electronic supplementary material, figure S5B), suggesting species differences in TMF expression (and potential downstream consequences for bleaching) are potentially affected by regulatory variation present within the HES2 locus.

It is interesting that both HES1 and HES2 contain divergent genes associated with the processing of misfolded proteins after heat stress. Similarly, the unfolded protein response pathway has been shown to be highly responsive to sub-bleaching heat exposure in corals (see [1]). If TMF ultimately is involved in regulating bleaching-related processes, it is possible that high expression of TMF could have opposite effects on bleaching depending on genetic background, given the observation that HE-like HES2 genotypes were associated with increased bleaching in HA, HC and HD (figure 2*c*). The mechanism of this possible epistasis would potentially reveal a great deal about the regulation of bleaching resistance. We cannot come to any concrete conclusions about the role of HES2 or TMF1 in coral bleaching from this study alone, but advocate for further study of their potential effects.

Our data shed light on reticulate evolution in corals [11]. Although HA, HC, HD and HE represent a monophyletic group compared to *A. millepora*, HE is more similar to *A. millepora* than any of the other cryptic species at HES1 and HES2. As a result, it is likely that the strong divergence of HES1 and HES2 in species HE is not owing to rapid evolution in species HE. Rather, this divergence is probably a reflection of differences between *A. hyacinthus* species HA, HC and HD versus *A. millepora*, and the strong similarity between HE and *A. millepora* in these specific parts of the genome. HES1 and HES2 might have introgressed into HE from a *millepora*-like coral at some point in the past after interspecific hybridization. Multiple amino acid changes at these loci in HA, HC and HD, without a signal of positive selection, as well as low expression of gene 12 599, might signal a change in function or lack of function at this locus in most *A. hyacinthus*. Alternatively, it may be that deeply divergent haplotypes have been circulating in the *hyacinthus* complex since its origin and have been maintained by long-term balancing selection, though this may be less likely for HES1, since it seems to be specific to HE. Similarly, the heat shock co-chaperone gene Sacsin has been pointed out as a highly polymorphic gene in *A. millepora*, perhaps maintained by balancing selection or introgression [19], although this gene has not been specifically linked to heat tolerance.

The linkage of SNPs in HES1 and HES2 along with their strong divergence is similar to other systems in which inversions harbour adaptive loci, prevent recombination and allow linked adaptive alleles to be passed to offspring [41,42]. One shortcoming of the low-coverage short-read approach used in this study is that it provides less information about the potential structural basis of regions showing elevated levels of genetic differentiation. Further studies using long reads and/or higher coverage would help clarify the role of structural variation in driving divergence among *A. hyacinthus* cryptic species.

(c) Evolutionary responses of cryptic species to climate change

Taken together, the ecology, heat resistance, symbiont choice, response to bleaching and genomic architecture of *A. hyacinthus* species HE all suggest that past adaptation to stressful microenvironments has prepared this species at least partially for the novel heat stress of climate change. Differences in resilience to the third global bleaching event in American Samoa could be largely explained by differential coral heat tolerance and symbiont associations. Adaptation to different thermal microenvironments appears to have proceeded rapidly, even in the recent past, given the phenotypic differences observed between cryptic species despite minimal

divergence across most of the genome. What can these results tell us about how *A. hyacinthus* will respond to future ocean warming? Because most of the genome-wide differences that define species HE are differences in allele frequencies, the relevant alleles are already present in the other cryptic species at low or moderate frequencies, and strong selection might increase their frequencies before these species go extinct [34]. However, the fitness consequences of these shifts might be contingent on the effects of more strongly divergent loci like HES1 (figure 3), or mitochondrial genotype (figure 1).

Our data add details about the genomic basis of such evolutionary shifts and raise the question of whether regions that are strongly differentiated between ecologically distinct cryptic species could also act as 'supergenes' that could help confer bleaching resilience. In this scenario, a bleaching resistance supergene might be passed via introgression, breeding or genetic engineering into the other cryptic species as ocean warming progresses and coral bleaching events become more common. In that case, non-HE individuals with HE-like haplotypes at divergent loci might be expected to show greater bleaching resilience. However, contrary to this expectation, we found that non-HE colonies that had HE-like genotypes at HES2 were *more* likely to be categorized as bleached. Although these results cannot conclusively determine the effects of HES2, or whether these effects differ according to the genomic background, they suggest caution in attempts to genetically engineer or hybridize corals for high heat tolerance. If genetic elements promoting heat tolerance in one species cause bleaching in a different genetic background, then moving genes between species may produce counter-productive results.

4. Methods

(a) Sample collection

In April and May 2015, we photographed and sampled branches from 62 previously identified and tagged coral colonies of *A. hyacinthus* in the HV and MV pools of Ofu, American Samoa [35,36]. We also identified, tagged and sampled 45 new colonies from these pools. We designated colonies for which more than 10% of the colony's area appeared to be bleached as 'bleached'. We stored samples in RNA-later at −20°C, then transported them to Stanford University for subsequent analyses. We also used archival samples from five colonies from August 2014 and two colonies from August 2011 for which we had bleaching observations but no tissue samples from 2015 (electronic supplementary material, table S1).

(b) Genome sequencing

We extracted genomic DNA using the Qiagen Allprep system and prepared samples for sequencing as described by Therkildsen & Palumbi [43]. Paired-end 125 bp Illumina sequencing genome sequencing was carried out across three lanes at the University of Utah Hunstman Cancer Institute; in addition to the 114 *A. hyacinthus* samples discussed here, 35 other samples of *Acropora gemmifera* were included in these lanes but are not discussed in the present study. Recent advances in the analysis of low-coverage sequencing data using genotype likelihoods allowed us to carry out a wide variety of population genomic analyses with this low-coverage data [44–47]. In particular, the use of the low-coverage-optimized population structure program *NGSadmix* allowed us to assign low-coverage samples to cryptic species [46]; once we had samples assigned to cryptic species we were able to carry out population-level analyses, e.g. windowed F_{ST} estimates using genotype likelihoods without hard-calling individual genotypes.

We used the *A. millepora* v. 2.01 genome to generate a '*hyacinthus*-ized' consensus genome [19]. First, we used *bwa mem* to map reads from a panel of 40 coral colonies (10 from each cryptic species, identified using *NGSadmix*) to the *A. millepora* genome using a map quality cutoff of 20 [48]. Then, we used *bcftools mpileup* and *bcftools consensus* to identify and apply to our reference 6 721 576 genetic variants where *A. hyacinthus* showed fixed differences from the *A. millepora* reference (1.4% divergence) [49]. The low level of divergence between *A. hyacinthus* and *A. millepora* suggests that the *A. millepora* reference should effectively serve as a reference for *A. hyacinthus*. The application of fixed *A. hyacinthus* variants increased the number of mapped reads by about 1% (from 741 076 617 to 763 684 010). We separately mapped reads to the *A. hyacinthus* mitochondrial genome (NCBI NC_022826). We used *pegas* to assemble mitochondrial haplotype networks [50]. We matched contigs from an earlier transcriptome study to predicted *A. millepora* transcripts using blastn (we used a one-way match rather than a reciprocal blast because some of the earlier contigs were fragmentary); all matches had an E-value less than 10^{-5}.

(c) Identification of cryptic species

We used *NGSadmix* with $k = 4$ to assign samples to the four previously identified cryptic species [46]; all samples were assigned to species with greater than 99.9% estimated ancestry. We categorized species as HA, HC, HD and HE using colonies that were present in this sample set and were also characterized by Ladner & Palumbi [23].

(d) Symbiont clade associations

We identified the proportion of symbiont clades C and D present in each sample by calculating the proportion of reads mapped (using *bwa mem* with map quality greater than 20) to previously published transcriptome references for clade C and clade D [51]. We calculated mean coverage across these references and calculated the proportion of clade D for each colony by dividing clade D coverage by the sum of mean coverage for both clades. We only included putative single-copy contigs with mean coverage across samples from 0.5 to 2× the median contig coverage.

(e) Identification of regions of high genomic divergence

We used *Angsd* to calculate pairwise F_{ST} at individual SNPs and in 10 kb windows between all pairs of cryptic species, only including sites with mean coverage of 1–4× across individuals; average F_{ST} within each window was calculated using the Fumagalli method using SNP sites with $p < 10^{-6}$ and MAF greater than 0.05 [52]. We then calculated the PBS from these F_{ST} estimates [53], using the formula $PBS = T1 + T2 - T3$, where $T = 1 - \log(F_{ST})$. T1 is calculated between the focal population and a closely related population, T2 between the focal population and an outgroup, and T3 between the related and outgroup populations. Because all four species were closely related in an approximate polytomy, we calculated the mean PBS value across the three possible combinations that could be used for each focal species. We used the R function *shuffle* from the package *permute* to implement a permutation test to detect regions showing greater divergence along each lineage than would be expected owing to random chance: we shuffled 10 kb windows across the genome 100 times, matching windows for mean π across species, and calculated an empirical cumulative distribution function for mean branch length in 100 kb windows with a 10 kb step. We calculated permutation *p*-values from our empirical cumulative distribution function and then identified 100 kb windows showing strong divergence in the HE lineage at FDR less than 0.05. We merged

100 kb outlier windows, identifying endpoints of outlier regions as stretching from the start position of the first 100 kb window to the end position of the last 100 kb window in uninterrupted adjacent sets of outlier windows with FDR less than 0.05.

In order to test the relative roles of reduced gene flow and selective sweeps in generating regions of differentiation, we calculated π_w (nucleotide diversity) and π_b (absolute divergence, or D_{xy}) across 10 kb windows using the *Angsd* program thetaStat and the program getDxy.pl from ngsTools (modified to skip sites that are not shared between species, available in the associated repository at github.com/noahrose) [47]. We normalized π_b and π_w to the number of bases with 1–4× mean coverage across samples in a given 10 kb window, calculated using *samtools depth*.

We used *PCAngsd* to carry out PCA of both genome-wide SNPs (SNP $p < 10^{-6}$ and MAF greater than 0.05) and the subset of those SNPs confined to specific divergent loci [54]. In each case, *PCAngsd* output a covariance matrix, which we used as input to the R function *eigen* to carry out PCA. We used *Angsd -doFasta 2* to generate consensus genomes for each cryptic species—this approach only output consensus sequence for regions that were covered by high-quality reads (MAPQ greater than 20) in at least one sample, preventing the consensus from defaulting to the '*hyacinthus*-ized' *A. millepora* reference sequence where sequence data was missing. We used *gffread* to generate predicted protein sequences from the consensus genomes. We used *phylogeny.fr* in 'one-click' mode to construct phylogenetic trees for proteins, and *bionj* from *ape* to construct neighbour-joining trees for HES1 and HES2.

We used a likelihood ratio test to test if cryptic species could explain additional variation in bleaching after accounting for symbiont association and pool of origin, as well as whether locus 2 could explain additional variation in bleaching after accounting for cryptic species, symbiont and pool of origin. We fitted a null binomial glm including these covariates using the R function *glm*. We then fitted a model including these covariates as well as PC1 across locus 2 and used to R function *anova*(type = 'Chisq) to carry out the likelihood ratio test. We also used the R function *anova* to test whether TMF expression was associated with PC1 across locus 2, including cryptic species as a covariate.

(f) Protein-coding analyses

We used *snpEff* to classify the protein-coding effects of variants that fell in protein-coding sequences [55]. We calculated population branch lengths, as described above in the windowed analyses, for each SNP. We used a permutation procedure to test whether nonsynonymous variants were more or less likely than synonymous variants to show lineage-specific shifts in allele frequency. We shuffled nonsynonymous and synonymous labels across SNPs and calculated the number of nonsynonymous variants reaching a specified PBS cutoff (top 10%, 5% and 1%). Because frequency spectra differed between synonymous and nonsynonymous variants (electronic supplementary material, figure S2A), we only shuffled labels among variants with the same MAF—in this way, we selected permuted sets of variants with the same frequency spectrum as our true set of nonsynonymous variants and tested how often they showed lineage-specific shifts in allele frequency, as measured by PBS. We also used Fisher's exact test, as implemented in R, to test whether fixed and polymorphic SNPs showed differences in the proportions of synonymous and nonsynonymous variants.

Data accessibility. The genome sequencing data are deposited in the NCBI SRA (accession PRJNA657822). Photographs of bleached and unbleached corals, scripts, and processed data are available at github.com/noahrose/114_coral_genomes.

Authors' contributions. N.H.R.: conceptualization, data curation, formal analysis, funding acquisition, investigation, methodology, project administration, validation, visualization, writing—original draft, writing—review and editing; R.A.B.: conceptualization, data curation, formal analysis, funding acquisition, investigation, methodology, project administration, writing—review and editing; M.K.M.: investigation, project administration, writing—review and editing; L.T.: data curation, investigation, project administration, writing—review and editing; E.A.S.: data curation, investigation, project administration, writing—review and editing; S.P.: conceptualization, data curation, formal analysis, funding acquisition, investigation, methodology, project administration, resources, supervision, validation, visualization, writing—original draft, writing—review and editing. All authors gave final approval for publication and agreed to be held accountable for the work performed therein.

Competing interests. The authors have no competing interests to declare.

Funding. This work was supported by grants from the Stanford Center for Computational, Evolutionary and Human Genomics, the Myers Trust and an NSF GRF to N.H.R.

Acknowledgements. We would like to thank Isabel Jones and Carlo Caruso for support in the field, and the National Park Service of American Samoa (permit no. NPSA-2015-SCI-0013).

References

1. Thomas L, Rose NH, Bay RA, LóPez EH, Morikawa MK, Ruiz-Jones L, Palumbi SR. 2018 Mechanisms of thermal tolerance in reef-building corals across a fine-grained environmental mosaic: lessons from Ofu, American Samoa. *Front. Mar. Sci.* **4**, 434. (doi:10.3389/fmars.2017.00434)
2. Brown BE. 1997 Coral bleaching: causes and consequences. *Coral Reefs* **16**, S129–S138. (doi:10.1007/s003380050249)
3. Hoegh-Guldberg O. 1999 Climate change, coral bleaching and the future of the world's coral reefs. *Mar. Freshw. Res.* **50**, 839–866. (doi:10.1071/MF99078)
4. Dixon GB, Davies SW, Aglyamova GV, Meyer E, Bay LK, Matz MV. 2015 Genomic determinants of coral heat tolerance across latitudes. *Science* **348**, 1460–1462. (doi:10.1126/science.1261224)
5. Jin YK, Lundgren P, Lutz A, Raina JB, Howells EJ, Paley AS, Willis BL, Van Oppen MJH. 2016 May 1 Genetic markers for antioxidant capacity in a reef-building coral. *Sci. Adv.* **2**, e1500842. (doi:10.1126/sciadv.1500842)
6. Bay RA, Palumbi SR. 2014 Multilocus adaptation associated with heat resistance in reef-building corals. *Curr. Biol.* **24**, 2952–2956. (doi:10.1016/j.cub.2014.10.044)
7. Oziolor EM, Reid NM, Yair S, Lee KM, Guberman Verploeg S, Bruns PC, Shaw JR, Whitehead A, Matson CW. 2019 May 3 Adaptive introgression enables evolutionary rescue from extreme environmental pollution. *Science* **364**, 455–457. (doi:10.1126/science.aav4155)
8. Jones MR *et al.* 2018 Jun 22 Adaptive introgression underlies polymorphic seasonal camouflage in snowshoe hares. *Science* **360**, 1355–1358. (doi:10.1126/science.aar5273)
9. Pardo-Diaz C, Salazar C, Baxter SW, Merot C, Figueiredo-Ready W, Joron M, Mcmillan WO, Jiggins CD. 2012 Jun 21 Adaptive introgression across species boundaries in *Heliconius* butterflies. *PLoS Genet.* **8**, e1002752. (doi:10.1371/journal.pgen.1002752)
10. Whitney KD, Randell RA, Rieseberg LH. 2010 Adaptive introgression of abiotic tolerance traits in the sunflower *Helianthus annuus*. *New Phytologist* **187**, 230–239. (doi:10.1111/j.1469-8137.2010.03234.x)
11. Mao Y, Economo EP, Satoh N. 2018 The roles of introgression and climate change in the rise to dominance of *Acropora* corals. *Curr. Biol.* **28**, 3373–3382. (doi:10.1016/j.cub.2018.08.061)
12. Tavares H *et al.* 2018 Oct 5 Selection and gene flow shape genomic islands that control floral guides.

Proc. Natl Acad. Sci. **115**, 11 006–11 011. (doi:10.1073/pnas.1801832115)

13. Turner TL, Hahn MW, Nuzhdin SV. 2005 Genomic islands of speciation in *Anopheles gambiae*. *PLoS Biol.* **3**, e285. (doi:10.1371/journal.pbio.0030285)
14. Wolf JB, Ellegren H. 2017 Making sense of genomic islands of differentiation in light of speciation. *Nat. Rev. Genet.* **18**, 87. (doi:10.1038/nrg.2016.133)
15. Schwander T, Libbrecht R, Keller L. 2014 Supergenes and complex phenotypes. *Curr. Biol.* **24**, R288–R294. (doi:10.1016/j.cub.2014.01.056)
16. Joron M *et al.* 2006 A conserved supergene locus controls colour pattern diversity in *Heliconius* butterflies. *PLoS Biol.* **4**, e303. (doi:10.1371/journal.pbio.0040303)
17. Smith J, Kronforst MR. 2013 Do *Heliconius* butterfly species exchange mimicry alleles? *Biol. Lett.* **9**, 20130503. (doi:10.1098/rsbl.2013.0503)
18. Barney BT, Munkholm C, Walt DR, Palumbi SR. 2017 Highly localized divergence within supergenes in Atlantic cod (*Gadus morhua*) within the Gulf of Maine. *BMC Genomics* **18**, 271. (doi:10.1186/s12864-017-3660-3)
19. Fuller ZL *et al.* 2020 Population genetics of the coral *Acropora millepora*: toward genomic prediction of bleaching. *Science* **369**, eaba4674.
20. Campbell CR, Poelstra JW, Yoder AD. 2018 What is speciation genomics? The roles of ecology, gene flow, and genomic architecture in the formation of species. *Biol. J. Linn. Soc.* **124**, 561–583. (doi:10.1093/biolinnean/bly063)
21. Baker AC, Glynn PW, Riegl B. 2008 Climate change and coral reef bleaching: an ecological assessment of long-term impacts, recovery trends and future outlook. *Estuarine Coastal Shelf Sci.* **80**, 435–471. (doi:10.1016/j.ecss.2008.09.003)
22. Hughes TP *et al.* 2017 Global warming and recurrent mass bleaching of corals. *Nature* **543**, 373. (doi:10.1038/nature21707)
23. Ladner JT, Palumbi SR. 2012 Extensive sympatry, cryptic diversity and introgression throughout the geographic distribution of two coral species complexes. *Mol. Ecol.* **21**, 2224–2238. (doi:10.1111/j.1365-294X.2012.05528.x)
24. Rose NH, Bay RA, Morikawa MK, Palumbi SR. 2018 Polygenic evolution drives species divergence and climate adaptation in corals. *Evolution* **72**, 82–94. (doi:10.1111/evo.13385)
25. Oliver TA, Palumbi SR. 2011 Many corals host thermally resistant symbionts in high-temperature habitat. *Coral Reefs* **30**, 241–250. (doi:10.1007/s00338-010-0696-0)
26. Baker AC, Starger CJ, Mcclanahan TR, Glynn PW. 2004 Coral reefs: corals' adaptive response to climate change. *Nature* **430**, 741. (doi:10.1038/430741a)
27. Gómez-Corrales M, Prada C. 2020 Cryptic lineages respond differently to coral bleaching. *Mol. Ecol.* **29**, 4265–4273. (doi:10.1111/mec.15631)
28. Prada C, Hellberg ME. 2013 Mar 5 Long prereproductive selection and divergence by depth in a Caribbean candelabrum coral. *Proc. Natl Acad. Sci.* **110**, 3961–3966. (doi:10.1073/pnas.1208931110)
29. Mcdonald JH, Kreitman M. 1991 Adaptive protein evolution at the Adh locus in *Drosophila*. *Nature* **351**, 652. (doi:10.1038/351652a0)
30. Lahti DC, Johnson NA, Ajie BC, Otto SP, Hendry AP, Blumstein DT, Coss RG, Donohue K, Foster SA. 2009 Sep 1 Relaxed selection in the wild. *Trends Ecol. Evol.* **24**, 487–496. (doi:10.1016/j.tree.2009.03.010)
31. Van Oppen MJH, Mcdonald BJ, Willis B, Miller DJ. 2001 Jul 1 The evolutionary history of the coral genus *Acropora* (Scleractinia, Cnidaria) based on a mitochondrial and a nuclear marker: reticulation, incomplete lineage sorting, or morphological convergence? *Mol. Biol. Evol.* **18**, 1315–1329. (doi:10.1093/oxfordjournals.molbev.a003916)
32. Gold Z, Palumbi SR. 2018 Long-term growth rates and effects of bleaching in *Acropora hyacinthus*. *Coral Reefs* **37**, 267–277. (doi:10.1007/s00338-018-1656-3)
33. Sheets EA, Warner PA, Palumbi SR. 2018 Accurate population genetic measurements require cryptic species identification in corals. *Coral Reefs* **37**, 1–15.
34. Cruickshank TE, Hahn MW. 2014 Reanalysis suggests that genomic islands of speciation are due to reduced diversity, not reduced gene flow. *Mol. Ecol.* **23**, 3133–3157. (doi:10.1111/mec.12796)
35. Tajima F. 1989 Nov Statistical method for testing the neutral mutation hypothesis by DNA polymorphism. *Genetics* **123**, 585–595. (doi:10.1093/genetics/123.3.585)
36. Fay JC, Wu CI. 2000 Jul 1 Hitchhiking under positive Darwinian selection. *Genetics* **155**, 1405–1413. (doi:10.1093/genetics/155.3.1405)
37. Traylor-Knowles N, Rose NH, Sheets EA, Palumbi SR. 2017 Early transcriptional responses during heat stress in the coral *Acropora hyacinthus*. *Biol. Bull.* **232**, 91–100. (doi:10.1086/692717)
38. Barnekow A, Thyrock A, Kessler D. 2009 Rab proteins and their interaction partners. *Int. Rev. Cell Mol. Biol.* **274**, 235–274. (doi:10.1016/S1937-6448(08)02005-4)
39. Papadopoulos N, Lennartsson J, Heldin C-H. 2018 PDGFRβ translocates to the nucleus and regulates chromatin remodeling via TATA element–modifying factor 1. *J. Cell Biol.* **217**, 1701–1717. (doi:10.1083/jcb.201706118)
40. Rose NH, Seneca FO, Palumbi SR. 2015 Gene networks in the wild: identifying transcriptional modules that mediate coral resistance to experimental heat stress. *Genome Biol. Evol.* **8**, 243–252. (doi:10.1093/gbe/evv258)
41. Jay P, Whibley A, Frezal L, Rodríguez de Cara MA, Nowell RW, Mallet J, Dasmahapatra KK, Joron M. 2017 Supergene evolution triggered by the introgression of a chromosomal inversion. *Curr. Biol.* **28**, 1839–1845e3.
42. Ayala D, Zhang S, Chateau M, Fouet C, Morlais I, Costantini C, Hahn MW, Besansky NJ. 2019 Mar Association mapping desiccation resistance within chromosomal inversions in the African malaria vector *Anopheles gambiae*. *Mol. Ecol.* **28**, 1333–1342. (doi:10.1111/mec.14880)
43. Therkildsen NO, Palumbi SR. 2017 Practical low-coverage genomewide sequencing of hundreds of individually barcoded samples for population and evolutionary genomics in nonmodel species. *Mol. Ecol. Res.* **17**, 194–208. (doi:10.1111/1755-0998.12593)
44. Buerkle C A, Gompert Z. 2013 Population genomics based on low coverage sequencing: how low should we go? *Mol. Ecol.* **22**, 3028–3035. (doi:10.1111/mec.12105)
45. Korneliussen TS, Albrechtsen A, Nielsen R. 2014 ANGSD: analysis of next generation sequencing data. *BMC Bioinf.* **15**, 356. (doi:10.1186/s12859-014-0356-4)
46. Skotte L, Korneliussen TS, Albrechtsen A. 2013 Estimating individual admixture proportions from next generation sequencing data. *Genetics* **195**, 693–702. (doi:10.1534/genetics.113.154138)
47. Fumagalli M, Vieira FG, Linderoth T, Nielsen R. 2014 ngsTools: methods for population genetics analyses from next-generation sequencing data. *Bioinformatics* **30**, 1486–1487. (doi:10.1093/bioinformatics/btu041)
48. Li H. 2013 Aligning sequence reads, clone sequences and assembly contigs with BWA-MEM. *arXiv*, 13033997.
49. Li H, Handsaker B, Wysoker A, Fennell T, Ruan J, Homer N, Marth G, Abecasis G, Durbin R. 2009 The sequence alignment/map format and SAMtools. *Bioinformatics* **25**, 2078–2079. (doi:10.1093/bioinformatics/btp352)
50. Paradis E. 2010 pegas: an R package for population genetics with an integrated–modular approach. *Bioinformatics* **26**, 419–420. (doi:10.1093/bioinformatics/btp696)
51. Ladner JT, Barshis DJ, Palumbi SR. 2012 Protein evolution in two co-occurring types of *Symbiodinium*: an exploration into the genetic basis of thermal tolerance in *Symbiodinium* clade D. *BMC Evol. Biol.* **12**, 217. (doi:10.1186/1471-2148-12-217)
52. Fumagalli M, Vieira FG, Korneliussen TS, Linderoth T, Huerta-Sánchez E, Albrechtsen A, Nielsen R. 2013 Quantifying population genetic differentiation from next-generation sequencing data. *Genetics* **195**, 979–992.
53. Yi X *et al.* 2010 Sequencing of 50 human exomes reveals adaptation to high altitude. *Science* **329**, 75–78. (doi:10.1126/science.1190371)
54. Meisner J, Albrechtsen A. 2018 Inferring population structure and admixture proportions in low-depth NGS data. *Genetics* **210**, 719–731. (doi:10.1534/genetics.118.301336)
55. Cingolani P, Platts A, Wang LL, Coon M, Nguyen T, Wang L, Land SJ, Lu X, Ruden DM. 2012 A program for annotating and predicting the effects of single nucleotide polymorphisms, SnpEff: SNPs in the genome of *Drosophila melanogaster* strain w1118; iso-2; iso-3. *Fly* **6**, 80–92. (doi:10.4161/fly.19695)